

Arrays of Josephson junctions in an environment with vanishing impedance

M. Aunola, J.J. Toppari and J.P. Pekola

Dept. of Physics, University of Jyväskylä, P.O. Box 35 (Y5), FIN-40351 Jyväskylä, Finland

(November 13, 2018)

The Hamiltonian operator for an unbiased array of Josephson junctions with gate voltages is constructed when only Cooper pair tunnelling and charging effects are taken into account. The supercurrent through the system and the pumped current induced by changing the gate voltages periodically are discussed with an emphasis on the inaccuracies in the Cooper pair pumping. Renormalisation of the Hamiltonian operator is used in order to reliably parametrise the effects due to inhomogeneity in the array and non-ideal gating sequences. The relatively simple model yields an explicit, testable prediction based on three experimentally motivated and determinable parameters.

I. INTRODUCTION

When a potential well propagates adiabatically along an electron system that is effectively one-dimensional, it carries with it additional electron density, and induces dc electric current through the system. Such a pumping effect has been studied in small metallic tunnel junctions in the Coulomb blockade regime.^{1,2} If the propagation of the potential well is arranged by phase-shifted gate voltages as in Refs. 1 and 2 and the potential well carries a quantised number n of electrons then the induced current I is related to the gating frequency f by the fundamental relation $I = -nef$, where $e = 1.602 \cdot 10^{-19}$ C. These Coulomb blockade pumps transporting single, normal-state electrons have reached accuracy suitable for metrological applications.^{2,3}

Until lately, mainly pumping of single electrons was studied, but in a recent article⁴ a quantitative theory of pumping Cooper pairs in gated one-dimensional arrays of Josephson junctions was presented. It was shown that quantum effects render the Cooper pair pump inaccurate in case of arrays with small junctions thus explaining the failure to demonstrate accurate pumping in the first (and so far the only) reported experiment of pumping of Cooper pairs.⁵

In this article, using renormalisation methods, we generalise the results derived in Ref. 4 for an unbiased array of Josephson junctions with gate voltages when only Cooper pair tunnelling and charging effects are taken into account. We consider the supercurrent, the higher order corrections for the pumping inaccuracy in case of homogeneous arrays, inhomogeneity of the array, and nonideal pumping sequences. Using three experimentally motivated and determinable parameters we are able to derive an expression for the pumping inaccuracy which can be directly compared against experimental results.

It should be stressed, though, that the model is simple and neglects many, possibly important features such as quasiparticle tunnelling, the coupling to the electromagnetic environment and the dissipative effects induced by a non-zero bias voltage. On the other hand, without these simplifications the problem could not be solved at the moment. The efficiency of the renormalisation methods in case of Cooper pair pumps is explained by the considerable symmetries of the model Hamiltonian. Renormalisation is widely used in atomic and nuclear physics,^{6–10} e.g. for the creation of effective two-body interactions used in nuclear Shell-Model calculations.

The article is organised as follows. In Secs. II and III the renormalisation method is explained and the expressions for the Hamiltonian as well as the charge transported by pumping are derived, respectively. In Sec. IV homogeneous arrays are examined in detail and in Sec. V the inhomogeneity is introduced. Finally in Sec. VI nonideal gating sequences are considered and the theoretical prediction for the pumping inaccuracy is explained thus leading to the conclusions in Sec. VII.

II. THE RENORMALISATION METHOD

A. Few-state dominant systems

Renormalisation methods may be applied most effectively in case of “few-state dominant” systems. In such systems some of basis states are separated from all the others by an energy ΔE which is large as compared to the coupling between any two states in the system. Thus certain eigenstates of the full system can be approximated by the eigenstates of the “few-state dominant” part only. Renormalisation can be described as a bridge spanning across the intervening gap.

For a given orthogonal basis $\{|l\rangle\}$ the Hamiltonian operator H can be written as

$$H = H_0 + V, \quad H_0|l\rangle = \epsilon_l|l\rangle, \quad l = 1, 2, \dots \quad (1)$$

where V is the residual interaction defining the coupling between eigenstates of H_0 . The matrix elements of V can often be considerably suppressed by a proper choice of the basis states. Explicitly, a part of the Hamiltonian can be called “ k -state dominant” if there are k basis states that satisfy the conditions

$$\begin{aligned} |\epsilon_l - \epsilon_m| &\geq \Delta E, & \text{if } l \leq k < m, \\ |V_{nn'}| &\ll \Delta E, & \text{for all } n, n'. \end{aligned} \quad (2)$$

The requirements of “few-state dominance” are graphically depicted in Fig. 1 showing some of the energy levels for two examples of a 5-state dominant system. Note that V_{\max} , the magnitude of the largest element in V , can be much smaller than the energy spread of the low-lying basis states.

B. The effective interaction

The aim of renormalisation is to generate an effective interaction \tilde{V} for a small, active space (P -space) which yields the same eigenvalues and eigenstates as the full Hamiltonian operator H . Similarly effective operators can be defined but this complication can be avoided in case of Cooper pair pumps. The renormalisation method in the context of nuclear physics is carefully explained in Refs. 6 and 7.

The effective interaction \tilde{V} for a k -dimensional P -space spanned by $\{|l\rangle\}_{l=1}^k$ can be derived as follows. One starts from the full Hamiltonian equation

$$H|\psi\rangle = E|\psi\rangle, \quad (3)$$

where E is an eigenvalue, inserts the expansion $|\psi\rangle = \sum_l a_l |l\rangle$ in order to obtain the set of linear equations for the coefficients $\{a_l\}$. In the first k equations of Hamiltonian the rest of the equations can be repeatedly applied in the form

$$a_{m(>k)} = \sum_{l=1}^k \frac{V_{ml} a_l}{E - \epsilon_m} + \sum_{m'(>k)} \frac{V_{mm'} a_{m'}}{E - \epsilon_m}. \quad (4)$$

The renormalisation eliminates coefficients $a_{m(>k)}$ and converges certainly if

$$\sum_{m'(>k)} \frac{|V_{mm'}|}{|E - \epsilon_m|} < 1 \quad (5)$$

for all states $|m\rangle$ with $m > k$. Inclusion of additional basis states in the P -space improves the convergence by reducing the number of coefficients that must be eliminated. Violation of the property (5) does not necessarily imply divergence, but the convergence should be checked more carefully.

We define operators $\hat{P} = \sum_{l=1}^k |l\rangle\langle l|$ and $\hat{Q} = \hat{1} - \hat{P}$ that project onto the P -space and the rest of the full space (Q -space), respectively. The renormalised Hamiltonian can then be written as

$$\tilde{H} = \hat{P}H_0\hat{P} + \tilde{V}. \quad (6)$$

where the effective interaction is given by

$$\tilde{V} = \hat{P} \left[\sum_{n=0}^{\infty} \left(V \frac{\hat{Q}}{E - \hat{Q}H_0\hat{Q}} \right)^n \right] V\hat{P}. \quad (7)$$

When \tilde{V} converges E is also an eigenvalue of renormalised Hamiltonian \tilde{H} which is manifestly consistent with the full Hamiltonian equation (3). But, unless \tilde{V} can be evaluated (analytically) up to the infinite order, the renormalisation should be truncated at a given order or when preset convergence criteria are met. This approximate effective interaction replaces \tilde{V} in Eq. (6).

The only remaining question is how the eigenenergy E should be chosen? The obvious, correct answer is “Insert E , get E' ”. The effective Hamiltonian \tilde{H} yields, allowing for convergence, k eigenvalues $\{\tilde{E}_j\}_{j=1}^k$. By repeatedly inserting an eigenvalue \tilde{E}_j into the definition of the effective interaction \tilde{V} we obtain the best available approximation for the eigenvalue $E_{[j]}$ of H as well as the renormalised eigenstates $|\tilde{j}\rangle$. A good initial guess is the eigenvalue $E_j^{(P)}$ of the pure P -space Hamiltonian $\hat{P}H\hat{P}$. We call this choice “individual” because the renormalisation has to be performed for each eigenstate in P -space separately.

The eigenstates $\{|\tilde{j}\rangle\}$ are not orthogonal in P -space because they correspond to different effective Hamiltonians, but if they are reexpanded to the full space the orthogonality can be regained. However, the requirements for “few-state dominance” ensure that the important advantage of orthogonality can be used in exchange for only a small loss in accuracy. In the “average” choice renormalisation, valid for “few-state dominant” systems, we use the average eigenenergy $\bar{E} = k^{-1} \sum_{j=1}^k \tilde{E}_j$ in place of individual eigenvalues. Thus the evaluation the diagonal matrix elements $\{\tilde{V}_{jj}\}$ suffices up until the final step of the iteration when H has to be diagonalised.

If the self-consistent iteration is not used we obtain the results directly corresponding to initial guesses. We refer to these cases as “individual-0” and “average-0” choices. These choices have been used since they often offer a more transparent interpretation of the result as well as much desired analytical results.

Finally we must emphasise that renormalisation and full diagonalisation in a restricted basis are just two similar although unidentical approaches to the eigenvalue problem. In renormalisation the full problem is projected onto a smaller space while in diagonalisation the problem is truncated by discarding all basis states outside the restricted basis.

III. THE COOPER PAIR PUMP

A. General properties

An array of Josephson junctions with gate voltages, a Cooper pair pump (CPP), in the Coulomb blockade regime is an excellent example of a few-state dominant system. In an earlier paper⁴ the leading component of the inaccuracy for transferred charge in a homogeneous

Cooper pair pump was derived. The higher order corrections to this leading order result are relatively insignificant in the immediate pumping regime. In that article the inaccuracy was evaluated from the variance of the number of Cooper pairs on an island far away from the island where most of the charge transfer occurs.

A crude version of the renormalisation process, amounting to “average-0” choice was also used in Ref. 4 for crosschecking the results. An analytical power expansion of the inaccuracy derived below was known as an “intelligent guess” but not included in the results. In addition, an analytical result for the pumped charge along a circular path for $N = 3$ on the gate voltage plane was derived by renormalisation.

Figure 2 shows a schematic drawing of a gated Josephson array of N junctions. Each junction has a capacitance C_k and a Josephson energy $E_{J,k}$. The phase difference over the array is $\phi \in [0, 2\pi N]$. It may be controlled by an external bias voltage V over the array according to the relation

$$\frac{d\phi}{dt} = \frac{(-2e)V}{\hbar}. \quad (8)$$

The oscillation frequency of ϕ is approximately $V [\mu\text{V}] \cdot 0.5 \text{ GHz}$, but all calculations in this article are done under an assumption of ideal zero bias ($V \equiv 0$) yielding a constant ϕ . Each gate voltage $V_{g,k}$ binds charge $C_{g,k}V_{g,k}$ on island k . In order to (hopefully) transport exactly one Cooper pair through the array the gate voltages are operated as depicted in Fig. 2. Thus the cycle consists of N legs and during k^{th} leg we expect one Cooper pair to tunnel through junction k .

There are two important energy scales in a CPP. The first one is the typical Josephson coupling energy E_J related to the Cooper pair tunnelling through the junctions and the second one is the charging energy E_C related to the charging effects of the small islands between the junctions. Both are explicitly defined below. The most important parameter of the model is the ratio E_J/E_C which will be denoted by ε_J .

B. The Hamiltonian and supercurrent operators

When we neglect the quasiparticle tunnelling and other degrees of freedom the model Hamiltonian is given by

$$H = H_C + H_J \quad (9)$$

where H_C is the charging Hamiltonian and H_J describes the Josephson tunnelling of the Cooper pairs. For an array of N junctions the tunnelling Hamiltonian has the form

$$H_J = - \sum_{k=1}^N E_{J,k} \cos \hat{\phi}_k \quad (10)$$

where $\hat{\phi}_k$ is the phase difference over the junction k , corresponding to a supercurrent operator

$$I_{S,k} = \frac{(-2e)E_{J,k}}{\hbar} \sin \hat{\phi}_k = \frac{-2e}{\hbar} \frac{\partial H_J}{\partial \hat{\phi}_k}. \quad (11)$$

The charging Hamiltonian H_C is diagonal in the basis formed by the charge eigenstates $|\vec{n}\rangle$ where $\vec{n} \equiv \{n_1, n_2, \dots, n_{N-1}\}$ and n_i is the number of Cooper pairs on each island of the array. The normalised gate voltages $\vec{q} \equiv \{q_1, q_2, \dots, q_{N-1}\}$ where $q_k = V_{g,k}C_{g,k}/(-2e)$ may be considered as parameters in H_C . The diagonal matrix elements are given by the classical charging energy

$$E_{\vec{n}} \equiv E_{\text{ch}}^{(\vec{n}, \vec{q})} = \sum_{k=1}^N \frac{Q_k^2}{2C_k} \quad (12)$$

where $Q_k = (-2e)v_k$ is the charge across the junction k . We define the typical charging energy of the array as $E_C = (2e)^2/2C$ where the “average” capacitance C is given by $C = N/\sum_{k=1}^N C_k^{-1}$ so that $C_k = c_k C$. The condition for ideal biasing yields $\sum_{k=1}^N v_k/c_k = 0$ and the conservation of charge on each island requires that

$$v_k - v_{k+1} = u_k \quad (13)$$

where $\vec{u} = \vec{n} - \vec{q}$. The unique solution satisfying these conditions is given by $v_k = \tilde{v}_k + y$ where

$$\tilde{v}_k = \sum_{j=k}^{N-1} u_j - \frac{1}{N} \sum_{j=1}^{N-1} j u_j, \quad y = -\frac{1}{N} \sum_{k=1}^N \frac{\tilde{v}_k}{c_k}. \quad (14)$$

By substituting the solution (14) into Eq. (12) we find

$$E_{\vec{n}} = E_C \left[\sum_{k=1}^N \frac{v_k^2}{c_k} - \frac{1}{N} \left(\sum_{k=1}^N \frac{v_k}{c_k} \right)^2 \right]. \quad (15)$$

where $v_k = \tilde{v}_k + \bar{y}$ for arbitrary \bar{y} since the expression (15) is invariant under the transformation $\{v_k\} \rightarrow \{v_k + \bar{y}\}$.¹¹ This symmetry can be effectively applied when renormalised matrix elements are evaluated.

The optimal basis for calculations is $\{|\vec{n}, \phi\rangle\}$, the basis of charge eigenstates augmented by the total phase difference over the array $\phi = \sum_{k=1}^N \phi_k$ which is periodic over $2N\pi$. The completeness of the basis was shown in case of normal-state electron systems by Ingold and Nazarov¹² who also give the canonical transformation between variables describing N separate junctions and variables describing $N - 1$ islands and the array as a whole. The conjugate phases on islands $\{\theta_k\}$ as well as the average number of tunnelled Cooper pairs $\mathcal{N} = (1/N) \sum_{k=1}^N m_k$ (m_k naturally corresponds to junction k) are completely undefined for the chosen basis states.

From now on we consider only the case when the phase difference over the array ϕ is kept fixed by ideal biasing and since ϕ is a constant of motion for the model Hamiltonian (9) we can explicitly write

$$H = H_C(\vec{q}) - \sum_{\vec{n}, k=1}^N \frac{E_{J,k}}{2} (|\vec{n} + \vec{\delta}_k\rangle\langle\vec{n}|e^{i\phi/N} + \text{H.c.}). \quad (16)$$

Here the tunnelling vector $\vec{\delta}_k$ describes the change of \vec{n} due to tunnelling of one Cooper pair through the k^{th} junction. The non-zero components of $\vec{\delta}_k$ are (if applicable) $(\vec{\delta}_k)_k = 1$ and $(\vec{\delta}_k)_{k-1} = -1$. Each tunnelling in the 'forward' direction is thus associated with a phase factor $e^{i\phi/N}$. The corresponding supercurrent operator is given by

$$I_{S,k} = \frac{(-2e)E_{J,k}}{2\hbar} \sum_{\vec{n}} (-i|\vec{n} + \vec{\delta}_k\rangle\langle\vec{n}|e^{i\phi/N} + \text{H.c.}) \quad (17)$$

where $I_{c,k} \equiv (-2e)E_{J,k}/\hbar$ is the critical current of junction k . We also define the (average) supercurrent operator I_S by

$$I_S = \frac{1}{N} \sum_{j=1}^N I_{S,j} = \frac{(-2e)}{\hbar} \frac{\partial H}{\partial \phi}. \quad (18)$$

The second equality follows from the ϕ -independence of H_C and the relation between ϕ_k and ϕ . The common expectation value of I_S and $I_{S,k}$ in a stationary state $|m\rangle$ is given by $(-2e/\hbar)\partial E_m/\partial\phi$ where E_m is the corresponding eigenenergy. Since I_S can be expressed as a derivative of the full Hamiltonian operator its matrix element between two different stationary states $|m\rangle$ and $|l\rangle$ can be expressed simply as

$$\langle m|I_S|l\rangle_\phi = \frac{(-2e)(E_m - E_l)}{\hbar} \lim_{\phi' \rightarrow \phi} \frac{\phi\langle m|l\rangle_{\phi'}}{\phi' - \phi}. \quad (19)$$

This expression is well-defined although one must keep track of the physically unimportant total phases of the wave functions.

C. The supercurrent and the transferred charge

As shown in the previous article⁴ there are two mechanisms of Cooper pair transfer in the array. The first one is the direct supercurrent flowing through the whole array due to non-zero ϕ and the other one is pumping, the charge transfer in response to the adiabatic variation of the injected charges \vec{q} .

The expressions for the charge transferred by these mechanisms can be derived as follows. For each instant of time t we introduce the basis of instantaneous eigenstates $\{|m_{(t)}\rangle\}$ with eigenenergies $\{E_m\}$ of the full Hamiltonian (9) for a given $\vec{q}(t)$. Assuming slowly varying gate voltages we may solve the time-dependent Schrödinger equation with the initial condition $|\psi(t_0)\rangle = |m_{(t_0)}\rangle$ to obtain

$$|\psi_{(t_0+\delta t)}\rangle = e^{-iE_m\delta t/\hbar} |m_{(t_0)}\rangle$$

$$+ \sum_{l(\neq m)} \frac{(e^{-iE_l\delta t/\hbar} - e^{-iE_m\delta t/\hbar}) \langle E_l | \vec{\nabla}_{\vec{q}} \rangle \cdot \frac{\partial \vec{q}}{\partial t} | l_{(t_0)} \rangle}{i(E_l - E_m)/\hbar} \\ \equiv |m_{(t_0)}\rangle + |\delta m_{(\delta t)}\rangle. \quad (20)$$

Here the term $|\vec{\nabla}_{\vec{q}}\rangle \cdot \frac{\partial \vec{q}}{\partial t}$ is the directional derivative of the ground state with respect to the change in gate charges \vec{q} . The amount of charge that passes through the junction k during a short time interval δt is then

$$\delta Q_k = \int_{t_0}^{t_0+\delta t} \langle \psi_{(t)} | I_{S,k} | \psi_{(t)} \rangle dt = \delta t \langle I_{S,k} \rangle_{|m_{(t_0)}\rangle} \\ + 2\text{Re} \left[\int_{t_0}^{t_0+\delta t} \langle m_{(t_0)} | I_{S,k} | \delta m_{(t-t_0)} \rangle dt \right], \quad (21)$$

where we have neglected the term quadratic in $|\delta m\rangle$ and oscillatory terms by assuming that $\delta t \gg \hbar/(E_l - E_m)$ holds for all l . The first term gives the charge transferred via direct supercurrent. The second term, the induced charge transfer, can be integrated yielding

$$\delta Q_{k,\text{ind}} = -2\hbar \sum_{l(\neq m)} \text{Im} \left[\frac{\langle m | I_{S,k} | l \rangle \langle l | \delta m \rangle}{E_l - E_m} \right] \quad (22)$$

where $|\delta m\rangle$ is the change in the instantaneous eigenstate induced by the change $\vec{q}(t_0) \rightarrow \vec{q}(t_0 + \delta t)$.

For a closed path γ the transferred charge must be equal for all N junctions so it can be written in terms of the average supercurrent operator I_S . The total amount of charge, Q , transferred over a pumping period τ is given by

$$\frac{Q}{-2e} = \frac{1}{\hbar} \int_0^\tau \frac{\partial E_m(t)}{\partial \phi} dt \\ - \frac{2\hbar}{-2e} \oint_\gamma \sum_{l(\neq m)} \text{Im} \left[\frac{\langle m | I_S | l \rangle \langle l | dm \rangle}{E_l - E_m} \right] \quad (23)$$

where $|dm\rangle$ is the differential change of $|m\rangle$ due to a differential change of the gate voltages $d\vec{q}$. It should be noted that the pumped charge depends only on the chosen path while the amount of charge transferred by direct supercurrent also depends on how the gate voltages are operated on the path. According to Eq. (19) the pumped charge for the state $|m\rangle$ simplifies to

$$\frac{Q_p}{-2e} = 2 \oint_\gamma \sum_{l(\neq m)} \text{Im} \left[\lim_{\phi' \rightarrow \phi} \frac{\phi \langle m | l \rangle_{\phi'}}{\phi' - \phi} \langle l | dm \rangle \right]. \quad (24)$$

Thus the pumped current is mediated by the induced mixing of other components into the initial state and modified depending on how the relative phases of the eigenstates change with respect to the differential change in ϕ . This formulation proves to be especially effective in the regime of two-state dominance. The operating frequency of gate voltages must satisfy $f \ll E_J/\hbar$ so that the adiabatic approximation is valid, though.

D. Numerical, renormalised and analytical results

In the following sections we refer to our results as numerical, renormalised or analytical. Numerical results are obtained by diagonalising the Hamiltonian operator (9) in a given basis and using the corresponding eigenstates in order to evaluate the required observable. The pumped charge Q_p is obtained by numerically integrating the second term in Eq. (23).

Renormalised results are obtained by a semianalytical process where the renormalised matrix elements in Eq. (7) for a given E are expressed analytically but the iteration process is naturally done numerically. Although restricting the analytical renormalisation into a given basis is quite difficult it facilitates direct comparison between the renormalised and numerically obtained results. Purely numerical renormalisation forfeits so much information that it is not used in this article.

The analytical results are obtained by renormalisation in such a manner that they can be expressed in a closed form. The analytical results for the supercurrent are given by the relation $(-2e/\hbar)\partial E_m/\partial\phi$ while the pumped charge is evaluated using Eq. (24).

IV. THE HOMOGENEOUS COOPER PAIR PUMP

A. The properties of the charging Hamiltonian

For uniform arrays all Josephson energies are equal to E_J and $c_k \equiv 1$ so the charging energy is given by

$$E_{\vec{n}} = E_C \left[\sum_{k=1}^N v_k^2 - \frac{1}{N} \left(\sum_{k=1}^N v_k \right)^2 \right], \quad (25)$$

provided that v_k are solutions of Eqs. (13). We shall now examine the properties and the symmetries of the charging Hamiltonian $H_C(\vec{q})$. Since the number of Cooper pairs on each island may obtain only integer values the degree of symmetry of $H_c(\vec{q})$ depends on how exactly the gate voltages \vec{q} match the set $\{\vec{n}\}$.

The most symmetrical case is obtained when $\vec{q} = \vec{n}_0$ for some charge eigenstate $|\vec{n}_0\rangle$. We then find $E_{\vec{n}_0} = 0$ and

$$E_{\vec{n}_0 \pm (\vec{s})} = E_C s(N-s)/N \quad (26)$$

where (\vec{s}) consists of s jumps through s different junctions in "forward" direction. Thus the Cooper pair pump is single-state dominant near the point of high symmetry and the supercurrent is given by $(-2e/\hbar)\partial V_{11}/\partial\phi$. The "average-0" choice now yields a supercurrent $I_C \cos(\phi)(N\varepsilon_J/2)^{N-1}N/(N-1)!$ in agreement with numerical results at $\vec{q} = \vec{n}_0$.

The degree of symmetry is almost as high on any line $\vec{n}_0 + x \cdot \vec{\delta}_r$ for any r and $x \in [0, 1]$. All junctions except the junction r are equivalent with respect to the charging

energy. In the region $x \approx 0.5$ the system is manifestly two-state dominant. This limit is the most relevant one for us since it is realised by ideal saw-tooth gating shown in Fig. 2.

The Hamiltonian is symmetric also at the so-called resonance point $\vec{q} = \vec{n}_0 + (1/N, \dots, 1/N)$, where the states $\{|\vec{n}_0 + \sum_{j=1}^k \vec{\delta}_j\rangle\}_{k=1}^N$ become degenerate. For N degenerate levels with nearest-neighbour coupling the ground state supercurrent is given by $I_{\text{res}}^{(0)}(\phi) \equiv I_C \sin(\phi/N)/N$ with $\phi \in (-\pi, \pi)$ exhibiting a cusp at $\phi = \pm\pi$. Because $\varepsilon_J > 0$ the coupling to the other states enhances the supercurrent which will be explicitly evaluated in Sec. IV C.

B. Pumping and supercurrent for homogeneous arrays

We will now evaluate the inaccuracy in the pumping for the uniform array when the gate voltages are operated as depicted in Fig. 2. Due to the symmetry of the charging Hamiltonian H_C it is enough to consider any one of the legs and multiply the results by N . In the Coulomb blockade regime for the saw-tooth gating cycle the system is always dominated by either one or two charge eigenstates. The pumping mainly occurs when these two states for each leg are nearly degenerate.

A two-level Hamiltonian can always be decomposed as

$$H = \begin{pmatrix} \epsilon_1 & ve^{-i\theta(\phi)} \\ ve^{i\theta(\phi)} & \epsilon_2 \end{pmatrix}. \quad (27)$$

For the truncated two-level system we have $\theta(\phi) = \phi/N$, $v = -E_J/2$ and $\epsilon_j = E_{\text{ch}}^{(j)}$, $j = 1, 2$. The proper decomposition of the renormalised Hamiltonian is

$$\tilde{H} \approx \begin{pmatrix} E_{\text{ch}}^{(1)} - a^{(1)} \cdot E_C & v|b(\phi)|e^{-i(\phi/N+\phi_b)} \\ v|b(\phi)|e^{i(\phi/N+\phi_b)} & E_{\text{ch}}^{(2)} - a^{(2)} \cdot E_C \end{pmatrix} \quad (28)$$

where $v = -E_J/2$, $a^{(j)} = a_0^{(j)} + a_1^{(j)} \cos \phi$, $j = 1, 2$, $b = b_0 + b_{-1}e^{-i\phi} + b_1e^{i\phi}$ and $e^{i\phi_b} = b/|b|$. The leading components for these coefficients are $a_0 \propto \varepsilon_J^2$, $a_1 \propto \varepsilon_J^N$, $b_0 \approx 1 + c\varepsilon_J^2$, $b_{-1} \propto \varepsilon_J^{N-2}$ and $b_1 \propto \varepsilon_J^N$. Thus \tilde{H} clearly tends to the unrenormalised Hamiltonian H in the natural limit $\varepsilon_J \rightarrow 0$.

The actual values for these parameters are discussed below. The next corrections in \tilde{H} are a_2 and $b_{\mp 2}$ which are further suppressed by a factor ε_J^N . The decomposition (28) is valid also for inhomogeneous Cooper pair pumps with only superficial changes. The renormalisation process itself is more complicated, though.

In the context of this two-level model the renormalisation coefficients a and b have the following interpretation. The diagonal coefficient a_0 corresponds to those tunnelling sequences that end in the same state inside the active P -space and without transporting any Cooper pairs through the array. Coefficients a_1 correspond to

those sequences that transport one Cooper pair in forward or backward direction, thus yielding the $\cos(\phi)$ -dependent term. The coefficients b arise from the sequences that connect the two charge eigenstates via the Q -space, transporting -1 , 0 or 1 Cooper pairs through the array. Each intermediate state $|\vec{n}\rangle$ naturally introduces an energy denominator $E - E_{\vec{n}}$.

This interpretation is illuminating and extremely helpful when evaluating the renormalisation coefficients but it has a very severe drawback. The picture we obtain is, unfortunately, false. The quantum mechanics implies that if $\varepsilon_J \neq 0$ all charge eigenstates simultaneously co-exist although the amplitude of most of these states is negligible in the low-lying eigenstates of the system. The renormalising sequences appear when we take into account the existence of high-lying states as described in Sec. II B.

In order to calculate the integral (24) for the leg in pumping we will use a parameter $\eta = (\epsilon_1 - \epsilon_2)/2v$ which is linear in the ascending gate voltage for the truncated system and almost linear for the renormalised system. The gating induced correction for the ground state yields a term $\langle 2|d1\rangle = \frac{1}{2}d\eta/(1+\eta^2)$ which is real. Thus we only need the imaginary part of the limit in (24) which reads

$$\text{Im} \left[\lim_{d\phi \rightarrow 0} \frac{\phi_0 \langle 1|2\rangle_{\phi_0+d\phi}}{d\phi} \right] = -\frac{d\theta/d\phi}{2\sqrt{1+\eta^2}}. \quad (29)$$

For the truncated system $d\theta/d\phi = 1/N$ and the pumped charge is given by

$$\frac{Q_p}{-2e} = \frac{1}{2N} \left[\frac{\eta_i}{\sqrt{1+\eta_i^2}} - \frac{\eta_f}{\sqrt{1+\eta_f^2}} \right]. \quad (30)$$

The symmetry of the full Hamiltonian (9) implies that the pumped charge for the full cycle should be exactly $-2e$ so we bluntly assume that the charge transfer in the limit $\theta \rightarrow \phi/N$ is exactly $Q_p = -2e$. We can partially justify this assumption by allowing for the missing charge transfer via higher excited states and noting that the identification of the initial and final states changes after each leg.

For the renormalised system $d\theta/d\phi$ may be evaluated analytically yielding

$$\frac{d\theta_{\text{ren}}}{d\phi} = \frac{1}{N} + \frac{b_0(-b_{-1} + b_1) \cos \phi - b_{-1}^2 + b_1^2}{|b(\phi)|^2}. \quad (31)$$

The pumping inaccuracy is then given by a weighted average of $Nd\theta/d\phi$ on a single leg. The weights can be obtained from Eq. (30) but for practical purposes it suffices to evaluate Eq. (31) at the degeneracy point. The coefficients are obtained by using the “average” choice for the eigenenergy E . In most cases the renormalisation includes all terms up to the third order and coefficients a_1 and $b_{\pm 1}$ up to and including order ε_J^N . The leading correction from $b_{-1} \cos \phi$ is proportional to ε_J^{N-2} as shown in Ref. 4.

In Fig. 3 the pumped charge Q_p for $N = 3$ is studied as function of the phase difference ϕ . The renormalised and numerical results are in good agreement and they clearly indicate that the deviations from the leading order result $(Q_p/(-2e)) = 1 - 9\varepsilon_J \cos \phi$ are important even when ε_J is relatively small. The maximum value for the numerical and renormalised pumped charges are 2.14 and 2.18, 2.87 and 2.98, 3.70 and 3.89 for $\varepsilon_J = 0.1, 0.15$ and 0.2, respectively.

Both minimum and maximum values of Q_p correspond to vanishing supercurrent which suggests that, in principle, the phase differences $\phi = 0$ and $\phi = \pi$ can be differentiated and the ratio $Q_{p,\text{max}}/Q_{p,\text{min}}$ could be used in order to determine ε_J . More realistic models are required in order to find out if this signature can persist when effects due to the electromagnetic environment are included.

In units E_C the renormalised eigenenergies read

$$\begin{Bmatrix} \tilde{E}_1 \\ \tilde{E}_2 \end{Bmatrix} = \frac{\epsilon_1 + \epsilon_2}{2} \mp \frac{1}{2} \sqrt{(\Delta\epsilon)^2 + \varepsilon_J^2 |b(\phi)|^2} \quad (32)$$

where $\Delta\epsilon = \epsilon_1 - \epsilon_2$. The ground state supercurrent is obtained by deriving \tilde{E}_1 with respect to ϕ with result

$$\begin{aligned} \langle I_S \rangle_{\text{g.s.}} = (I_c \sin \phi) & \left[\frac{a_1^{(1)} + a_1^{(2)}}{2\varepsilon_J} \right. \\ & \left. + \frac{b_0(b_{-1} + b_1) + 2b_{-1}b_1 \cos \phi - (a_1^{(1)} - a_1^{(2)})\Delta\epsilon/\varepsilon_J}{(2/\varepsilon_J)\sqrt{(\Delta\epsilon)^2 + \varepsilon_J^2 |b(\phi)|^2}} \right]. \end{aligned} \quad (33)$$

In Fig. 4 the renormalised and numerical supercurrents are shown for $N = 5$. The renormalisation using the “individual” choice reproduces the supercurrent well in all three cases. For clarity a basis with 40 states was used although it is not large enough to produce the leading order (ε_J^{N-1}) supercurrent fully. The slight underestimation of the supercurrent at the degeneracy point is explainable since we could use only leading order terms in the renormalisation. Below we study various effects related to restricted bases.

C. The basis-dependent effects

In order to reliably evaluate the pumped charge or the supercurrent one must first select a proper basis in which the calculations are performed. The basis should be as large as possible so that the discarded states are not important but on the other hand such calculations may require prohibitive amounts of CPU-time. Our aim is to circumvent these problems by using renormalisation techniques.

Numerical calculations have been mainly performed in three classes of bases we refer to as a-, b- and c-bases. From here on we reserve the superscript in parenthesis $^{(k)}$ for the ε_J^k -dependent part of any coefficient and the distinction between charge eigenstates 1 and 2 is taken to

be complied implicitly. An a-basis contains all states contributing to the leading order inaccuracy ($b_{-1}^{(N-2)}$) while a b-basis produces the leading component of the supercurrent ($b_1^{(N)}$) fully. Even larger c-basis contains all states required for the next-to-leading correction of the inaccuracy ($b_{-1}^{(N)}, b_1^{(N)}$).

For each length of the array N these bases can be created as follows. The leading component of the inaccuracy (supercurrent) is carried by the $N-1$ -step (N -step) “paths” containing at most one tunnelling through each junction that connect the initial state to the final state (itself) for each leg. The total number of necessary states is $2^{N-2}N$ and $2^{N-1}N$ for an a-basis and a b-basis, respectively. A short reasoning confirms that a state should be included in a c-basis if it can be reached from some state in the corresponding b-basis by a single tunnelling. The number of states has not been generally resolved but in cases $N = 4$ to $N = 8$ the c-basis contains 100, 325, 966, 2695 and 7176 states.

The numerical evaluation of the pumping integral in Eq. (23) may require up to 10^5 to 10^6 complete diagonalisations per leg before convergence is obtained which is extremely time-consuming for bases containing more than few hundred basis states. The supercurrent has been evaluated even for the $N = 8$ c-basis since only one eigenstate is needed. Due to computational necessities some modifications of the above-mentioned bases have been used.

The differences between bases can be illuminated by performing an “average-0” choice renormalisation at the degeneracy point of the saw-tooth gating path. Inserting the coefficients $b_j^{(k)}$ ($j = 0, \pm 1$) and respective powers of ε_J into Eq. (31) one obtains a power expansion of the inaccuracy for small values of ε_J . This expansion has to be corrected for the drop in ground state energy induced by the terms $a_0^{(k)}$.

In order to include all contributions up to the next-to-leading order ε_J^N we need the expressions for coefficients $a_0^{(2)}, b_0^{(2)}, b_{-1}^{(N-2)}, b_{-1}^{(N)}$ and $b_1^{(N)}$. Simple expressions are obtained for

$$\begin{aligned} a_{0,a}^{(2)} &= \frac{N-2}{4} + \frac{N(N-1)}{4(N-2)}, \\ a_{0,b+}^{(2)} &= \frac{N-1}{4} + \frac{N(N-1)}{4(N-2)} + \frac{N}{4(2N-2)}, \\ b_{0,a}^{(2)} &= N/2, \\ b_{0,b+}^{(2)} &= N(N-1)/2(N-2), \\ b_{-1,a+}^{(N-2)} &= \left(\frac{N}{2}\right)^{N-2} \frac{N-1}{(N-2)!} \end{aligned}$$

where index a and b corresponds to a- and b-bases and + implies that coefficient does not change when basis is enlarged. The analytical expressions for the coefficients $b_{-1}^{(N)}$ and $b_1^{(N)}$ are composed of several multiple summations. The obtained values of $b_{-1}^{(N)}$ for different bases and $b_1^{(N)}$ for c-basis are given in Table I.

The power expansion of the pumped charge then reads

$$\begin{aligned} \frac{Q_p}{-2e} &\approx 1 - N\varepsilon_J^{N-2} \cos \phi \left[b_{-1}^{(N-2)} \right. \\ &\quad \left. + \varepsilon_J^2 \left(b_{-1}^{(N)} - b_1^{(N)} - (Nl(N)a_0^{(2)} + b_0^{(2)})b_{-1}^{(N-2)} \right) \right] \end{aligned} \quad (34)$$

where $l(N) \approx 1$ stems from the energy denominators. Its value is 1, 1, 11/12, 5/6 and 137/180 in cases $N = 3$ to $N = 7$, respectively. For $N = 3$ and $N = 4$ the strong deviations from $\cos(\phi)$ -dependence are explained by additional terms $27(\varepsilon_J \cos \phi)^2 - 81(\varepsilon_J \cos \phi)^3$ and $24\varepsilon_J^4 \cos^2 \phi$, respectively. The expansion (34) for $N = 3$ does not compare too well against numerical results in Fig. 3 but inclusion of the above-mentioned terms improves agreement considerably up to $\varepsilon_J \approx 0.1$.

Next we take a closer look at the case $N = 5$ in Fig. 5 where the power expansions for the b-basis and the 240-state basis (almost full c-basis¹³) as well as the results for “average” renormalisation are compared to numerical results for $\phi = 0$. The inaccuracy is given in units ε_J^3 which allows more detailed comparison of the predictions. The renormalised values follow the numerical results more closely than the power expansions but the differences between bases are still reproduced well up to $\varepsilon_J \approx 0.1$. In addition the inaccuracy for a-basis is correctly placed in between these bases.

Similar overestimation can be seen in the inset of Fig. 5 showing the numerical and renormalised inaccuracies for $N = 7$. Although the results may not seem to be so good at the first glance, one should bear in mind that the 336-states basis for which the convergence is the best corresponds to even smaller an inaccuracy than the $N = 7$ b-basis. Actual inaccuracy should be evaluated for much larger c-basis which is, unfortunately, clearly impossible. The scaling of the inaccuracy by ε_J^5 certainly exaggerates the error, too. In conclusion we may state that the renormalisation seems to be able to reproduce the behaviour of the inaccuracy reasonably well for any N and ε_J in the Coulomb blockade regime.

The enhancement of the supercurrent at the resonance point has been studied but the conclusions remain valid also in its vicinity. For small values of ε_J next-to-nearest neighbour coupling yields approximate supercurrent $1 + N\varepsilon_J \cos(\phi/N)$ in our units of choice, $I_{\text{res}}^{(0)}(\phi)$. In the more general case have used semianalytical third order renormalisation with $2N(N-1)$ state P -space and compared the results to the supercurrent obtained by diagonalisation.

For $\phi \approx \pi$ and $6 \leq N \leq 10$ and the comparison is shown in Table II clearly indicating that the differences between bases for $\varepsilon_J = 0.1$ are not significant but for $\varepsilon_J = 0.2$ they are growing. The renormalisation calculations indicate that for $\varepsilon_J = 0.1$ the convergence is fast both with respect to the order of renormalisation as well as the basis. As conclusion we may state that the enhancement is important for large N and ε_J although it will not cancel the overall suppression $\sim 1/N^2$ of the maximal supercurrent.

V. INHOMOMOGENEITY IN THE ARRAY

In this section we will derive the leading contributions for the pumping inaccuracy and the supercurrent on the saw-tooth gating path for an inhomogeneous array. General considerations imply that the quantity $E_J E_C$ is approximately constant for all junctions in an array. The Josephson energy is inversely proportional to the normal state resistance R_T of the junction and E_C is inversely proportional to the capacitance C of the junction. Since R_T is inversely proportional and C is directly proportional to the area of the junction, the product is approximately constant for different junctions in the array. (This argument works for junctions fabricated in the same batch; otherwise the constants of proportionality are different.)

The model Hamiltonian (9) is uniquely defined by the ratio ε_J and relative capacitances $\{c_k\}_{k=1}^N$ once we set $E_{J,k} = c_k E_J$ in the tunnelling Hamiltonian H_J . We define the inhomogeneity index of the array

$$X_{\text{inh}} = \left(\frac{1}{N} \sum_{k=1}^N g_k^2 \right)^{1/2} \quad (35)$$

where $g_k = 1/c_k - 1$ in order to study the behaviour of the inaccuracy as a function of X_{inh} . Although the definition is valid for arbitrary X_{inh} the limits $X_{\text{inh}} < 0.15$ and $|g_k| < 0.5$ are reasonable for the current technology at capacitances of the order of 1 fF.

On r^{th} leg of the gating cycle the initial and final states are $|\vec{n}_r\rangle$ and $|\vec{n}_r + \vec{\delta}_r\rangle (|\vec{n}_{r+1}\rangle)$, respectively. The gate voltages are given by $\vec{q} = \vec{n}_r + x\vec{\delta}_r$ where $x \in [0, 1]$ is the normalised ascending gate voltage so that $x = \frac{1}{2}$ corresponds to the degeneracy point. In order to obtain the leading order contributions for the inaccuracy and supercurrent we must set $a_0 = 0$, $b_0 = c_r$ in the renormalised Hamiltonian (28) and evaluate coefficients a_1 and b_{-1} .

All the required states on the r^{th} leg can be chosen from the classes $|\vec{n}_r \pm (\vec{s})\rangle$ for $s = 0, 1, \dots, N-1$ where (\vec{s}) defined in Sec. IV A does not contain $\vec{\delta}_r$. Let σ denote a permutation of the set $\{1, 2, \dots, N\} \setminus \{r\}$, $\sigma(s)$ the set of s first elements in σ and σ_k the k^{th} element of σ .¹⁴ Each $\sigma(s)$ then defines two states with charging energies

$$E_{\pm s,x} \equiv E_{\vec{n}_r \pm (\vec{s})}(x, \sigma) = \frac{E_C}{N} \left[(N/c_r - 1/c_r^2) x^2 + (s + G_\sigma^s) ((N-s) \pm 2x(1+g_r) - G_\sigma^s) \right] \quad (36)$$

where $G_\sigma^s = \sum_{k=1}^s g_{\sigma_k}$. The charging energies for the initial and final states are given by $E_{0,x}$ and $E_{0,1-x}$, respectively.

The leading order of pumped charge can be obtained for the “average-0” choice at the degeneracy point for each leg yielding result

$$\frac{Q_p}{-2e} = 1 - (K \cos \phi) \sum_{r=1}^N \sum_{\sigma} \frac{c_r^{-2}}{\prod_{s=1}^{N-2} \Delta E_{-s,\sigma}}, \quad (37)$$

exact in the limit $\varepsilon_J \rightarrow 0$. Here $K \equiv \left(\frac{NE_J}{2E_C} \right)^{N-2} \prod_{k=1}^N c_k$ and

$$\begin{aligned} \Delta E_{-s,\sigma} &\equiv (N/E_C)(E_{-s,\frac{1}{2}} - E_{0,\frac{1}{2}}) \\ &= (s + G_\sigma^s)(N - s - 1 - g_r - G_\sigma^s). \end{aligned} \quad (38)$$

The analytical result (37) gives us the theoretical ratio between inhomogeneous and homogeneous inaccuracy which will be denoted by W_{inh} and compared to numerical results. The interpretation is obvious since for small values of ε_J the higher order corrections are not very important and even then their behaviour is relatively similar to the leading contribution.

The inaccuracy is invariant under arbitrary permutations of the set $\{c_k\}$. Numerically the pumped charge may be evaluated for any of the N junctions but far better numerical convergence is obtained by using the average supercurrent operator I_S . The total inaccuracy for an inhomogeneous array is always larger than the corresponding homogeneous array and the junctionwise inaccuracy for $c_k > 1$ ($c_k < 1$) is smaller (larger) than average inaccuracy.

In Fig. 6 W_{inh} is plotted as function of X_{inh} corresponding to some specific sets of relative capacitances $\{c_k\}$ for $N = 4$ and $N = 5$. The numerical results have been obtained for b-bases. The agreement between analytical and numerical results is good showing that the effects due to inhomogeneity of the array can be reliably treated as a correction factor when relative capacitances c_k are given.

The effects due to inhomogeneity can be parametrised by obtaining limits for W_{inh} as a function of X_{inh} . For $X_{\text{inh}} = |g|$ this is achieved by considering the even distribution of inhomogeneity ($g_{\text{odd}} = g$, $g_{\text{even}} = -g$ for even N and $g_{\text{odd}} = g \left(\frac{N-1}{N+1} \right)^{1/2}$, $g_{\text{even}} = g \left(\frac{N+1}{N-1} \right)^{1/2}$ for odd N) yielding a lower limit and maximally distorted distribution ($g_1 = g\tilde{N}$, $g_{k(\geq 2)} = g/\tilde{N}$, $\tilde{N} = \sqrt{N-1}$) corresponding to an upper limit. The upper limit yields a simple, analytical result

$$W_{\text{inh}}(X_{\text{inh}}, N) \leq \max[f(X_{\text{inh}}, N), f(-X_{\text{inh}}, N)] \quad (39)$$

where

$$\begin{aligned} f(g, N) &= \frac{[1 - g/\tilde{N}]^{5-3N}}{N(1 + g\tilde{N})} \left[(1 + g\tilde{N})^2 \right. \\ &\quad \left. + (1 - g/\tilde{N})^2 \sum_{k=1}^{N-1} \left[\prod_{s=N-k}^{N-2} \frac{s}{s+\gamma} \prod_{s=k}^{N-2} \frac{s}{s+\gamma} \right] \right] \end{aligned} \quad (40)$$

with $\gamma = Ng/(\tilde{N} - g)$. The analytical expression for the lower limit is obtained by explicitly inserting the even distribution in Eq. (37) and using the symmetry in order to reduce the number of terms to be calculated. Even simpler a lower limit can be obtained by considering the asymptotical behaviour of the inhomogeneity. We find

$$W_{\text{inh}}(X_{\text{inh}}, N) \geq 1 + a_N^{(\text{inh})} X_{\text{inh}}^2 \quad (41)$$

where the N -dependent constant $a_N^{(\text{inh})}$ can be evaluated from Eq. (40) yielding values 8, 85/9, 1279/20, 42317/3600, 40267/3150, and 13.769 for cases $N = 4$ to $N = 9$, respectively.¹⁶ In Fig. 7 we graphically present the limits for $(W_{\text{inh}} - 1)/X_{\text{inh}}^2$ as function of X_{inh} in cases $N = 4$ to $N = 7$. For $X_{\text{inh}} = 0.15$ we obtain limits 20 %, 24 %, 28 % and 32 % as the maximal increase in inaccuracy as compared to the homogeneous case for $N = 4$ to $N = 7$, respectively.

The leading order renormalised supercurrent may be evaluated using the "individual-0" choice as follows. The eigenenergies of the truncated Hamiltonian are

$$\begin{aligned} \tilde{E}_1 \\ \tilde{E}_2 \end{aligned} \left\{ \right. = \frac{E_{0,x} + E_{0,1-x}}{2} \mp \frac{1}{2} \sqrt{\Delta_{0,x}^2 + c_r^2 E_r^2} \quad (42)$$

where $\Delta_{0,x} = E_{0,x} - E_{0,1-x}$. Using \tilde{E}_1 in the renormalisation now yields the leading order supercurrent $I_{r,x} \equiv \langle I_S \rangle_{(r,x)}$, on leg r for ascending gate voltage x as

$$I_{r,x} = \sum_{\sigma} \sum_{l=1}^N \frac{(I_c \sin \phi) (E_J/2)^{N-1} \prod_{k=1}^N c_k}{\left(\prod_{m=1}^{l-1} \Delta E_{\sigma}^{(m)} \right) \left(\prod_{m=l}^{N-1} \Delta E_{\sigma}^{(r,m)} \right)} \quad (43)$$

where energy differences are given by $\Delta E_{\sigma}^{(s)} = E_{s,x} - \tilde{E}_1$, for $s = 1, \dots, N-1$ and $\Delta E_{\sigma}^{(r,s)} = E_{\bar{s},x} - \tilde{E}_1$, $\bar{s} = -(N-s-1)$ corresponding to the last elements of σ . From Eq. (33) we find $\Delta E_{\sigma}^{(r,0)} = \tilde{E}_2 - \tilde{E}_1$ for the remaining energy difference. In Fig. 8 the analytical prediction (43) is compared against and numerically evaluated supercurrent for $N = 6$ b-basis. Each curve corresponds to a randomly chosen set $\{c_k\}$ $\varepsilon_J \in [0.02, 0.06]$ as seen from the different widths of the peak. The numerical and analytical results practically coincide.

Finally, by using (43) we can explain the a -basis supercurrent in Fig. 4. For a homogeneous array $g_k \equiv 0$ and the charging energies $E_{\pm s,x}$ are identical so the summation over σ yields a prefactor $(N-1)!$. The omission of certain states amounts to disallowing some paths and the numerator has to be corrected by a factor $(l-1)/(N-1)$ which is exactly how the supercurrent for a -basis can be evaluated.

VI. THE PUMPING INACCURACY AND NONIDEAL GATING

In this section we will derive the leading order correction induced by nonideal gating sequences which we define below. When all gate voltages are turned off in Fig. 2 in beginning of the first leg the actual gate voltages can be expressed as $\vec{q}_{(1)} = \vec{n}_1 + \vec{q}_{\text{off}}$ defining the $N-1$ offset errors. The maximum values of the normalised sweeping voltages are given by $q_{\text{sw},k} = 1 + \hat{q}_{\text{sw}}^{(k)}$ whence the initial gate voltages on k^{th} leg read

$$\vec{q}_{(k>1)} = \vec{n}_k + \vec{q}_{\text{off}} + \hat{q}_{\text{sw}}^{(k-1)} \vec{\Delta}_{k-1} \quad (44)$$

where $\vec{\Delta}_k = \sum_{j=1}^k \vec{\delta}_k$. In general, the sweeping voltages can be determined more precisely than the offset voltages, and for most of our calculations we have used 1 % and 2 % precisions for them, respectively.

As in the case of inhomogeneity we can determine the effects due to nonideal gating sequences provided we can evaluate the charging energy differences at the degeneracy point. On the r^{th} leg we choose the coordinates of the degeneracy point as

$$\vec{q}_{(\text{deg},r)} = \vec{n}_r + \frac{1}{2} \vec{\delta}_r + \sum_{j=1}^N \mu_j \vec{\delta}_j \quad (45)$$

thus defining quantities μ_j subject to condition $\mu_r = 0$. The degeneracy condition $E_{\vec{n}_r} = E_{\vec{n}_{r+1}}$ can be solved easily yielding

$$\sum_{j=1}^N (\mu_j / c_j) = 0. \quad (46)$$

Thus on each leg one must find where the line connecting the initial and final gate voltages crosses the hyperplane defined by Eq. (46). This clearly implies that the correct nonideality parameter is

$$X_{\text{non}} = \left[\frac{1}{N} \sum_{\text{leg}=1}^N \sum_{j=1}^N \left(\frac{\mu_j^{(\text{leg})}}{c_j} \right)^2 \right]^{1/2} \quad (47)$$

which can easily be evaluated once the offset and sweeping voltages are given.

The leading order inaccuracy may be evaluated using the charging energies (15) at the degeneracy point and inserting the corresponding energy differences (multiplied by N/E_C) into Eq. (37). Dividing the result by the inaccuracy for a homogeneous array and ideal gating sequence we obtain the ratio W_{non} . We are mainly interested in the behaviour of W_{non} for very small values of X_{non} so we have only evaluated the asymptotical limit

$$W_{\text{non}} \sim 1 + a_N^{(\text{non})} X_{\text{non}}^2 \quad (48)$$

for homogeneous array. Here $a_N^{(\text{non})}$ is given by 40/3, 1225/108, 41/4, 258181/27000, 6136/675 in cases $N = 4$ to $N = 9$, respectively.

In order to show that X_{non} really is the correct parameter we chose several sets of offset and sweeping voltages for homogeneous arrays. We then evaluated W_{non} both analytically and numerically for $N = 4$ a-basis with $\varepsilon_J = 0.05$ and $N = 5$ a-basis with $\varepsilon_J = 0.04$. The results are shown in Fig. 9 which also show the asymptotic limits. Theoretical values lie on the curves as well as most of the numerical data points.

The full inaccuracy may be approximately understood in terms of the contribution from the inhomogeneity and nonideality. In order to show this we have used nonideal gating sequences with some of the inhomogeneous

arrays already used in Fig. 6. We have collected the results in Table III which includes the parameters X_{inh} and X_{non} and numerical ratio W_{non} as compared to the full theoretical correction and product of corrections due to pure inhomogeneity and pure nonideality. The reasonable agreement between theoretical and numerical results shows that we really can take into account both inhomogeneity and nonideal gating sequences.

Finally we must note that since the connection between X_{non} and offset and sweeping voltages is much more complicated than the connection between relative capacitances and X_{inh} , there is no straightforward way to obtain X_{non} from the experimental data. An approximate upper limit can be given easily, though. A sort of worst-case scenario for $|q_{\text{off},k} + \tilde{q}_{\text{sw}}^{(k)}| < x_{\text{non}}$ when the precision of the gating for each component is known, yields

$$X_{\text{non}}(N) \approx \frac{x_{\text{non}}(14 + 11N + 4N^2 + N^3)^{1/2}}{6^{1/2}N} \quad (49)$$

which can be used in Eq. (48) and combining this result with the estimated limits for X_{inh} one obtains reasonable limits for the ratio W_{non} . Multiplying W_{non} by the inaccuracy corresponding to homogeneous array and ideal gating, allowing for indeterminacy of ε_J , finally yields the final prediction of the present model. The prediction, based on these three parameters, is a range inside which the inaccuracy is expected to lie, but it remains to be seen whether the electromagnetic environment or other effects strongly modify the present results.

VII. CONCLUSIONS

We have studied pumping of Cooper pairs for an unbiased array of Josephson junctions in an environment with vanishing impedance. The present model, which includes only charging effects and Cooper pair tunnelling, can be reliably solved yielding relatively simple predictions for the direct supercurrent and the accuracy of the pumping of Cooper pairs.

We have successfully evaluated higher order corrections for the supercurrent as well as the pumping inaccuracy for ideal gating sequence and homogeneous arrays. The effects due to inhomogeneous arrays or nonideal gating sequences can be quantitatively treated by defining parameters X_{inh} and X_{non} and respective correction factors W_{inh} and W_{non} .

The parameters ε_J and X_{inh} can be experimentally measured and the precision of the gate voltages yields limits for X_{non} so the present model can give an explicit prediction for the expected range of the experimental inaccuracy. The theoretical predictions have been verified by numerical calculations, but whether the model is realistic enough to give quantitatively, or least qualitatively correct results will be ultimately tested in experiments. In any case, further theoretical studies using more realistic and sophisticated models should be performed.

¹ H. Pothier, P. Lafarge, C. Urbina, D. Esteve and M.H. Devoret, *Europhys. Lett.* **17**, 249 (1992).

² M.W. Keller, J.M. Martinis, N.N. Zimmerman and A.H. Steinbach, *Appl. Phys. Lett.* **69**, 1804 (1996); M.W. Keller, J.M. Martinis and R.L. Kautz, *Phys. Rev. Lett.* **80**, 4530 (1998).

³ M.W. Keller, Ali L. Eichenberg, John M. Martinis and Neil M. Zimmerman, *Science* **285**, 1716 (1999).

⁴ J.P. Pekola, J.J. Toppuri, M. Aunola, M.T. Savolainen and D.V. Averin, *Phys. Rev. B* **60**, R9931 (1999).

⁵ L.J. Geerligs, S.M. Verbrugh, P. Hadley, J.E. Mooij, H. Pothier, P. Lafarge, C. Urbina, D. Esteve and M.H. Devoret, *Z. Phys. B: Condens. Matter* **85**, 349 (1991).

⁶ P.J. Ellis and E. Osnes, *Rev. Mod. Phys.* **49**, 777 (1978).

⁷ M. Hjorth-Jensen, in *Advances in Quantum Many-Body Theory*, Vol. 2, eds. R. Bishop and N.R. Walet, (World Scientific, Singapore), in press.

⁸ M. Hjorth-Jensen, T.T.S. Kuo and E. Osnes, *Physics Reports* **261** 125 (1995).

⁹ T.T.S. Kuo and E. Osnes, *Folded-Diagram Theory of the Effective Interaction in Atomic Nuclei*, Springer Lecture Notes in Physics, (Springer, Berlin, 1990) Vol. **364**; T.T.S. Kuo, *Lecture Notes in Physics; Topics in Nuclear Physics*, eds. T.T.S. Kuo and S.S.M. Wong, (Springer, Berlin, 1981) Vol. **144**, p. 248.

¹⁰ I. Lindgren and J. Morrison, *Atomic Many-Body Theory*, *J. Phys. B: At. Mol. Opt. Phys.* **24** (1991) 1143.

¹¹ The charging energy differences in the presence of an external bias are unaffected for a homogeneous array. The charging energy differences only deviate from those given by (15) for an inhomogeneous array with an external bias.

¹² G.-L. Ingold and Yu. V. Nazarov, in *Single Charge Tunnelling, Coulomb Blockade Phenomena in Nanostructures*, eds. H. Grabert and M.L. Devoret, (Plenum Press, New York), 1992.

¹³ The 240-state basis and some of the data was created when the authors worked on Ref. 4. Since calculations are take a lot of CPU-time and the value of $b_{-1}^{(N)}$ for this basis is just 2 % short of the full c-basis value we chose to fill the missing data rather than adopt the c-basis.

¹⁴ The notation $\{1, 2, \dots, N\} \setminus \{r\}$ stands for the set of all positive integers up to N excluding r .

¹⁵ Our calculations show that the inaccuracies can be predicted even on a “leg by leg”-basis but since legwise inaccuracies can not be measured they can not be considered as results. In addition, the agreement is better for the full cycle.

¹⁶ The lower limit in Fig. 7 is not valid in the strict, mathematical sense but the violation is extremely weak and it only occurs for $X_{\text{inh}} \leq 0.03$. The asymptotical limit (41) is never violated, though.

TABLE I. The coefficients $b_{-1}^{(N)}$ for a-, b- and c-basis and $b_1^{(N)}$ for c-basis in cases $N = 3$ to $N = 9$ obtained by using “average-0” choice renormalisation at the degeneracy point. Exact values are given as fractions when the value fits into the column.

N	$b_{-1,a}^{(N)}$	$b_{-1,b}^{(N)}$	$b_{-1,c}^{(N)}$	$b_{1,c}^{(N)}$
3	9/4	57/8	69/8	3/4
4	63/2	436/10	513/10	5/2
5	83.189	106.44	125.54	5.792
6	176.78	217.07	261.52	459/40
7	339.51	405.5	497.62	20.834
8	—	—	894.45	35.781
9	—	—	1544.9	59.135

TABLE II. The maximal supercurrent ($\phi \approx \pi$) in units $I_{\text{res}}^{(0)}(\phi)$ for relatively long arrays and strong coupling. For different bases the results were obtained by diagonalisation and the renormalised value is for third order renormalisation and $2N(N - 1)$ -state P -space.

N	ε_J	a-basis	b-basis	c-basis	renorm
6	0.1	1.485	1.488	1.491	1.492
6	0.2	1.881	1.897	1.913	1.914
7	0.1	1.589	1.591	1.596	1.601
7	0.2	2.072	2.087	2.113	2.117
8	0.1	1.689	1.691	1.697	1.708
8	0.2	2.256	2.271	2.303	2.316
9	0.1	1.786	1.788	—	1.815
9	0.2	2.435	2.448	—	2.508
10	0.1	1.881	1.883	—	1.923
10	0.2	2.601	2.621	—	2.690

TABLE III. The ratios W_{non} corresponding to nonideal gating in an inhomogeneous array. The numerical values $W_{\text{non, num}}$ have obtained by numerical integration for $N = 5$ a-basis with $\varepsilon_J = 0.04$ or b-basis with $\varepsilon_J = 0.03$. The values of $W_{\text{non, ren}}$ and $W_{\text{non, prod}}$ are obtained by renormalisation when inhomogeneity and nonideal gating sequences are treated simultaneously and separately, respectively.

X_{inh}	X_{non}	$W_{\text{non, num}}$	$W_{\text{non, ren}}$	$W_{\text{non, prod}}$
0.0131	0.0377	1.0178	1.018	1.018
0.0263	0.0130	1.0082	1.0085	1.0085
0.0292	0.0173	1.0095	1.0115	1.0115
0.0387	0.0163	1.0169	1.0173	1.0173
0.0515	0.0174	1.0277	1.0287	1.0289
0.0541	0.0244	1.0339	1.0346	1.0349
0.0653	0.0237	1.0463	1.048	1.0477
0.0741	0.0201	1.0572	1.0577	1.058
0.0783	0.0315	1.0697	1.0706	1.0714

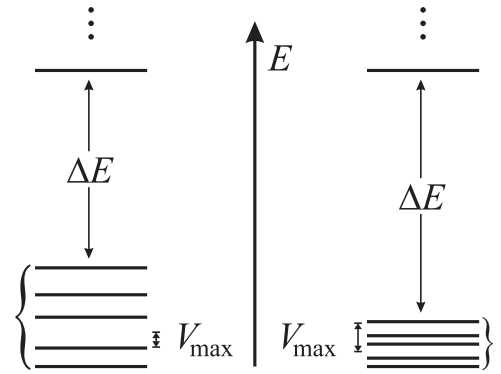


FIG. 1. Schematic view of two possible 5-state dominant systems. On the right-hand-side all low-lying levels are closely packed in energy while on the left-hand-side the spread is large as compared to V_{max} . In both cases the requirements for few-state dominance are well satisfied.

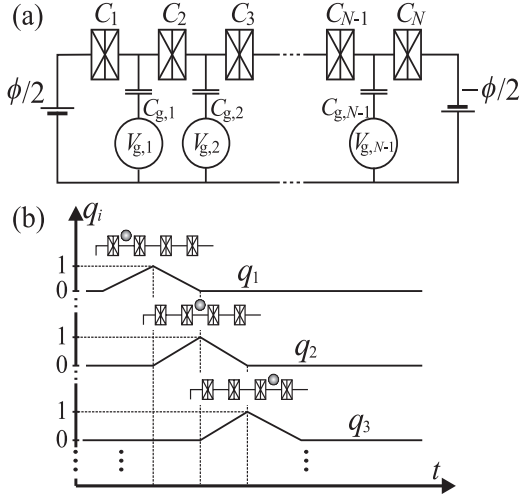


FIG. 2. (a) A schematic drawing of a gated Josephson array of N junctions. In pumping Cooper pairs, gate voltages $V_{g,k}$ are operated cyclically. C_k are the capacitances of the junctions and $C_{g,k}$ are the gate capacitances. b) A train of gate voltages to carry a charge in a pump. Here $q_k = -C_{g,k}V_{g,k}/2e$. The dominant state at the turning points of gate voltages are also shown.

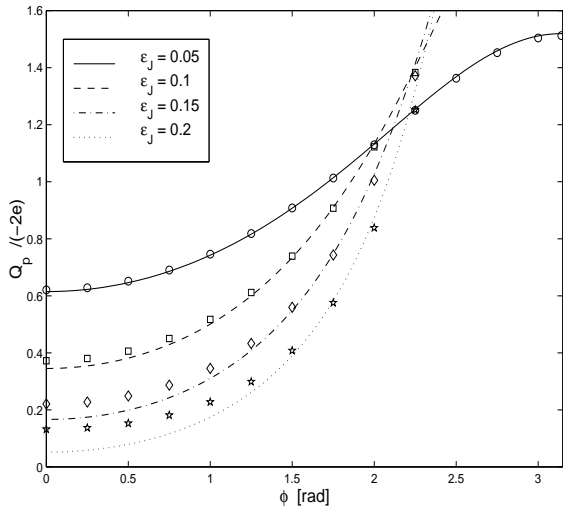


FIG. 3. The pumped charge $Q_p/(-2e)$ as a function of ϕ for some values of ϵ_J and $N = 3$. Curves denote renormalised values and symbols numerical values which were obtained for a 41-state basis. Pumped charge is symmetric in ϕ and its period is 2π .

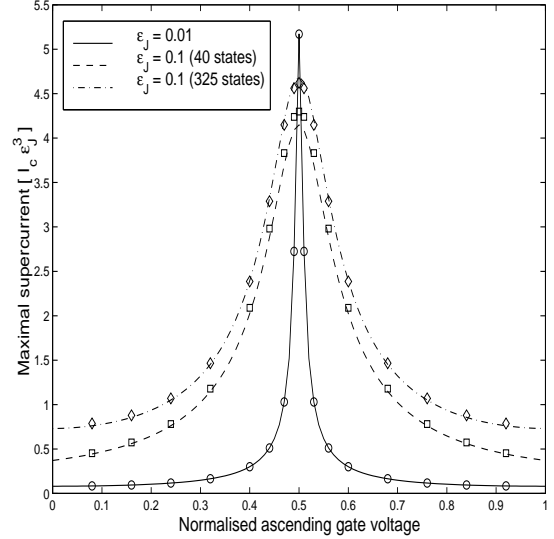


FIG. 4. The maximal value for the supercurrent in units $I_C \epsilon_J^3$ for $N = 5$. Curves denote renormalised values and symbols numerical values corresponding to bases with 40 and 325 states. In case $\epsilon_J = 0.01$ the differences between bases can hardly be seen even at the degeneracy point.

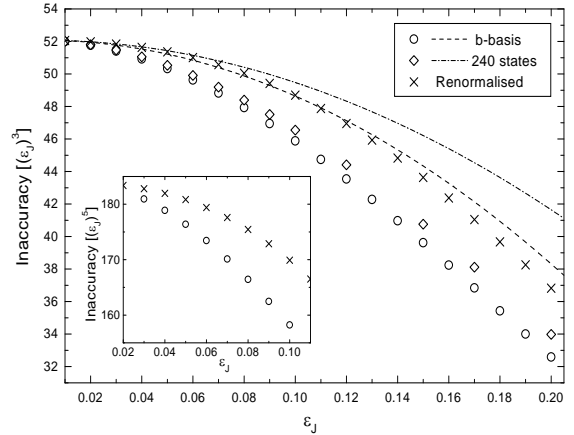


FIG. 5. The inaccuracy of the pumped charge $Q_p/(-2e)$ as a function of ϵ_J for different bases and $N = 5$. Curves denote analytical power expansions and symbols numerical or renormalised values. The inaccuracy is given in units ϵ_J^3 and the phase difference used is $\phi = 0$. Inset shows the corresponding results for the $N = 7$, 336-state basis.

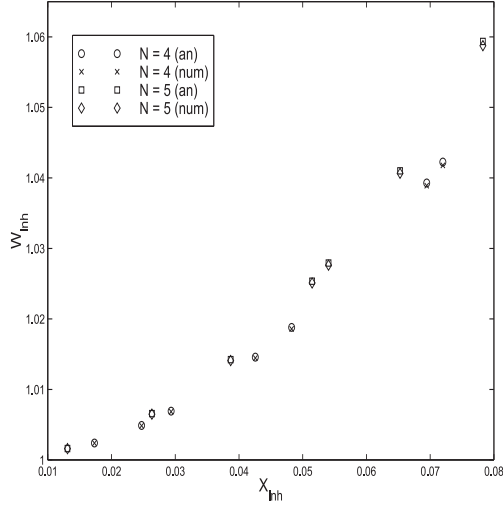


FIG. 6. The ratios W_{inh} between the inhomogeneous and the homogeneous inaccuracies from analytical expression (37) and numerical calculations as functions of the inhomogeneity index X_{inh} which is defined in Eq. (35). Numerical results were obtained for b-bases with $\varepsilon_J = 0.02$ and $\varepsilon_J = 0.03$ for $N = 4$ and $N = 5$, respectively.

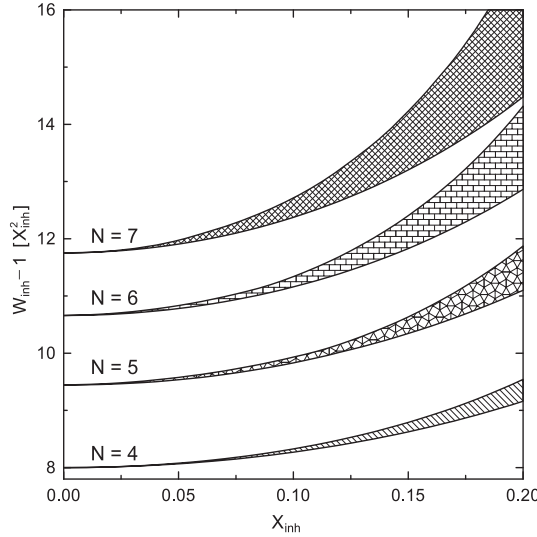


FIG. 7. The limits for the ratio W_{inh} as a function of X_{inh} for array lengths $N = 4$ to $N = 7$. For small values of X_{inh} $W_{\text{inh}} \approx 1 + a_N^{(\text{inh})} \cdot X_{\text{inh}}^2$ which allows several cases to be presented simultaneously.

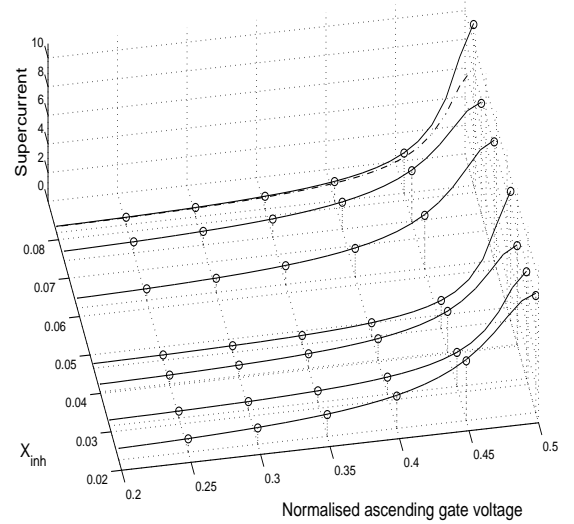


FIG. 8. A three-dimensional plot of the maximal supercurrent for $N = 6$ c-basis in units $I_c \varepsilon_J^4$ for several sets $\{c_k\}$ corresponding to different X_{inh} . The gate voltages are chosen from the first leg of the saw-tooth gating path. Junction capacitances have been chosen randomly as well as the ratios ε_J which lie between 0.02 and 0.06. Solid curves denote analytical values and discrete symbols numerical values. The modifications of the supercurrent are well reproduced even for larger inhomogeneities. The dash-dot curve represents the homogeneous supercurrent the largest $X_{\text{inh}}..$

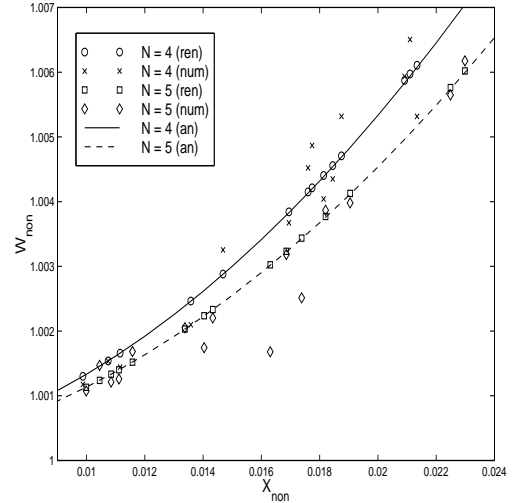


FIG. 9. W_{non} for homogeneous arrays and nonideal gating sequences as function of X_{non} . The renormalised values are almost identical to the asymptotical expansions (48) shown as lines. Numerical values agree reasonably well with theoretical results. We used a-bases with $\varepsilon_J = 0.05$ and $\varepsilon_J = 0.04$ for $N = 4$ and $N = 5$, respectively.